Theor Chem Acc (2004) 112: 263–269
DOI 10.1007/s00214-004-0586-z

Theoretical
Chemistry Accounts

Regular article

Rotational cooling of $Li_2(^1\Sigma_g^+)$ molecules by ultracold collisions with a helium gas buffer

E. Bodo[1], **F. A. Gianturco**[1], **F. Sebastianelli**[1], **E. Yurtsever**[2], **M. Yurtsever**[3]

[1]Department of Chemistry and INFM, University of Rome "La Sapienza", P. A. Moro 5, 00185, Rome, Italy
[2]Department of Chemistry, Koç University, Istanbul, Turkey
[3]Department of Chemistry, Technical University of Istanbul, Turkey

Received: 17 July 2003 / Accepted: 18 December 2003 / Published online: 16 June 2004

Abstract. The very weak interaction of Li_2 with He atoms has been obtained from accurate ab initio calculations and is here analyzed in terms of its anisotropic features. Quantum scattering calculations of the rotational inelastic de-excitation cross sections are carried out using a recently proposed multichannel treatment, the modified variable phase method, implemented by the authors and applied here to ultralow collision energies. General conclusions on the low efficiency of a He buffer gas in cooling down molecular rotations in this system are presented and analyzed.

Keywords: Molecular collisions – Ultralow energy scatterring – Vibrational collisional cooling – Van de-Waals interaction forces – Atom–molecule quantum scattering

1 Introduction

The last few years have witnessed a very rapidly growing interest, both experimental and theoretical, in the the field of cold molecules [1, 2, 3, 4, 5]. Such a marked growth has been inspired by the spectacular results which have been achieved in the closely related area of cold atoms where Bose–Einstein condensation (BEC) in dilute gases of alkali atoms has been obtained. Although molecules are a much more difficult working environment for BEC experiments, it has been clear from the very beginning that they have much more to offer that simply providing an extension of the sort of experiments already performed with atoms. Cold and ultracold molecules have therefore attracted the interest of both the chemical and the physical communities in trying to better understand the large variety of additional effects that are likely to take place at very low temperatures. There are currently three experimental methods which are employed to produce cold molecules that can be trapped for a time long enough to be further manipulated. One of the most widely used approaches starts with cold atoms stored in a magneto-optical trap and, through the process of photoassociation, binds two atoms together [6,7]. The ensuing molecules are translationally as cold as the atoms from which they are produced but, since the latter get together at rather large internuclear distances, the most favored states of the molecules formed are often high vibrational states just below their dissociation limit. Using a variety of laser schemes, the internal energy distributions of the newly formed molecules can be manipulated in order to transfer them into their ro-vibrational and electronic ground states. In the second method, a beam of dipolar molecules is decelerated during the passage through an array of time-varying inhomogeneous electric fields and then trapped in an electrostatic storage ring [5] or in an electrostatic quadrupole trap [8]. Another possibility for cooling molecules is offered by injecting them in a cold He buffer [9, 10] where they can then thermalize after a series of multiple collisions. When ^{3}He is used as a buffer gas, the temperature can be as low as 250 mK and one can still maintain a sufficient buffer gas density to ensure efficient cooling by frequent collisions. It is therefore of importance to have some previous knowledge of the relative sizes and for the corresponding collisionally inelastic cross sections related to a particular molecule injected in the buffer gas to initiate the cooling step of the process. This essentially means that to gather theoretical information on the inelastic collisions occurring at ultralow temperatures we have to have previously acquired reliable information on the anisotropic interactions which drive the collisional cooling. In the present study we will present a new and fairly reliable description of the interaction of Li_2 with the He atom that has

Proceedings of the 11th International Congress of Quantum Chemistry satellite meeting in honor of Jean-Louis Rivail

This work is affectionately dedicated to Prof. Jean-Louis Rivail on the occasion of his university retirement. We wish our friend many more happy years of research and the continued opportunity of guiding young scientists.

Correspondence to: F. A. Gianturco
e-mail: fa.gianturco@caspur.it

been computed in our group and employ it to analyze the relative efficiency of collisionally cooling rotational states of that diatomic target.

2 The rigid rotor potential

The potential energy surface (PES) was computed in Jacobi coordinates by fixing the internuclear distance of the Li_2 molecule at its equilibrium value of 2.7 Å. The extension of the computations to other Li_2 geometries is currently in progress and will be analyzed elsewhere. We believe, however, that the present computed interaction should be accurate enough to reliably perform the studies described later, since we do not expect any significant modification of the Li_2 bond length due to the approaching of one He atom, a very weak perturber of the molecule as we shall see later. Furthermore, the quantum structures of Li_2 in small ^{4}He clusters are also likely to affect very little its equilibrium bond length and therefore can be realistically studied with the present rigid rotor (RR) surface.

The ab initio calculations were done via Gaussian98 [11], using the quadratic configuration interaction with singles, doubles and noniterative corrections due to triples (QCISD(T)) with a correlation- consistent polarized-valencte quadratic zeta basis set and with a frozen lithium core. Each of the calculated points was counterpoise-corrected to avoid the basis set superposition errors (BSSE) that turned out to be very large in this system. The calculations were repeated for selected geometries with the coupled-cluster method with singles, doubles and noniterative corrections due to triples (CCSD(T)) with the same basis set: the results of the QCISD(T) and the CCSD(T) are almost exactly the same within 10^{-6}%. Another set of selected geometries was repeated without freezing the lithium core. No more than 2–3% differences were detected between computations done with or without a frozen core.

Since the interaction between the molecule and the atom is highly isotropic, only four orientations were computed and for each of them 35 different R values were obtained. The potential-energy curves corresponding to the four angles are reported in Fig. 1. As one can see, this is a very weak interaction and its minimum geometry turns out to be linear, a feature that we shall further discuss later in more detail. It is worth noting at this point that the isotropic interaction between atomic Li and He has a maximum depth of 1.5 cm^{-1}[12] (one of the strongest among those existing in the alkali-helium pairs). The interaction that we obtain in the Li_2–He system turns out to be smaller, by a factor of 2, that that of the atomic case. This effect is probably due to the presence of interaction forces which now describe a potential between two closed-shell systems (Li_2 and He) while the atomic radical structure produced more efficient dispersion contributions. The molecular interaction is essentially isotropic and the minimum distance moves from 7.6 to 6.9 Å, i.e., only about 10% when going over the whole angular range. The fact that the anisotropy of this interaction is very small is further confirmed when one looks at the usual multipolar expansion coefficients $V_\lambda = \frac{2\lambda+1}{2}\int_{-1}^{1} V(R,\theta)P_\lambda(\cos\theta)\mathrm{d}\cos\theta$ that we found to numerically converge rapidly and to require a relatively small number of λ values to accurately reproduce the original points of the RR surface. As a pictorial example, the first two terms of the V_λ expansion are reported in the inset of Fig. 1.

As far as we know, all the PESs calculated before for the title system were either semiempirical or obtained by

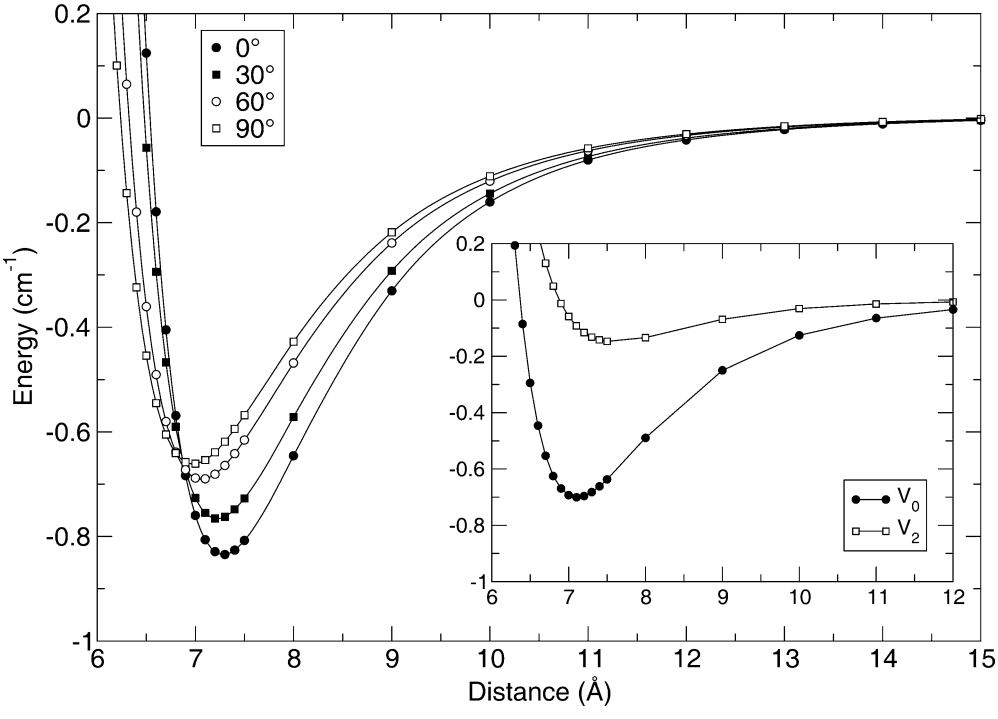

Fig. 1. Computed points of the interaction once corrected for basis set superposition errors as a function of R and for four different orientations. The *inset* reports the first two expansion term V_0 and V_2

fitting preexisting but old ab initio calculations. However, we shall pursue in this section a comparison with these earlier data in order to get a better feeling for the overall reliability of our results. A comparison between the repulsive part of the potential calculated by us and the semi empirical one obtained by Rubahn [13] is reported in Fig. 2. The agreement of the repulsive region of the potential is actually very good. Larger differences still exist, however, in the attractive region of the potential. We therefore report a comparison between three potentials in Fig. 3: the potential obtained here, that from the fitting of Rubahn[13] and the one obtained by Fuchs and Toennies[14] as a fitting of unpublished Configuration Interaction calculations. The $\theta = 0^\circ$ and $\theta = 90^\circ$ orientations are reported. The potentials obtained by Rubahn (dashed lines) are weaker with respect to ours for both orientations, while the minimum values are larger than those obtained by us. This may be due to a underestimation of the C_n coefficients used in Ref. [13] to model the long-range part of the potentials since they were obtained by second-order perturbation theory. The potential of Fuchs and Toennies presents instead well regions which are much deeper than ours and this may be caused by the lack of a proper correction for

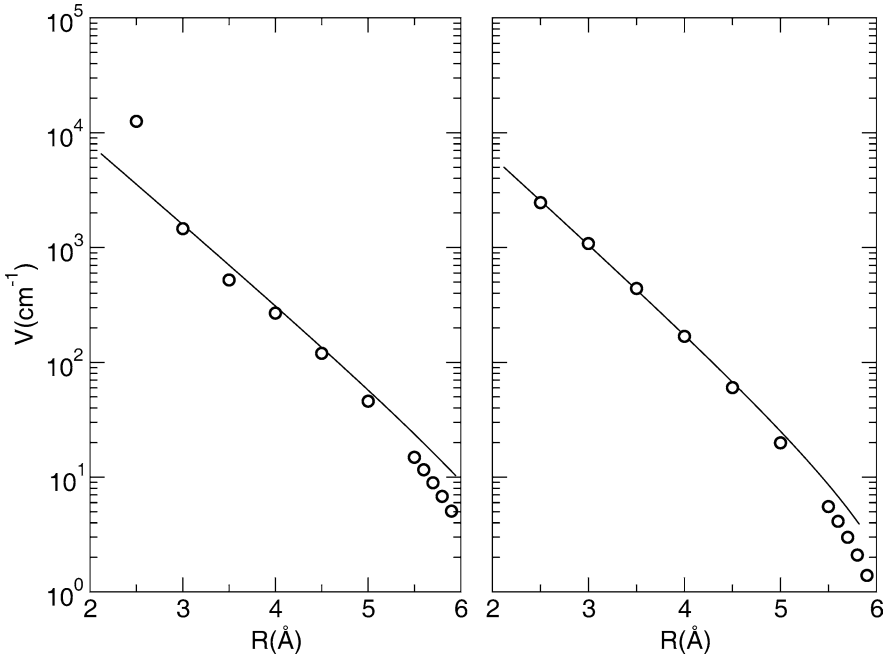

Fig. 2. Comparison of the repulsive part of the potential: *circles* present work, *solid line* from Ref. [13]. *Left panel* for $\theta = 0^\circ$, *right panel* for $\theta = 90^\circ$

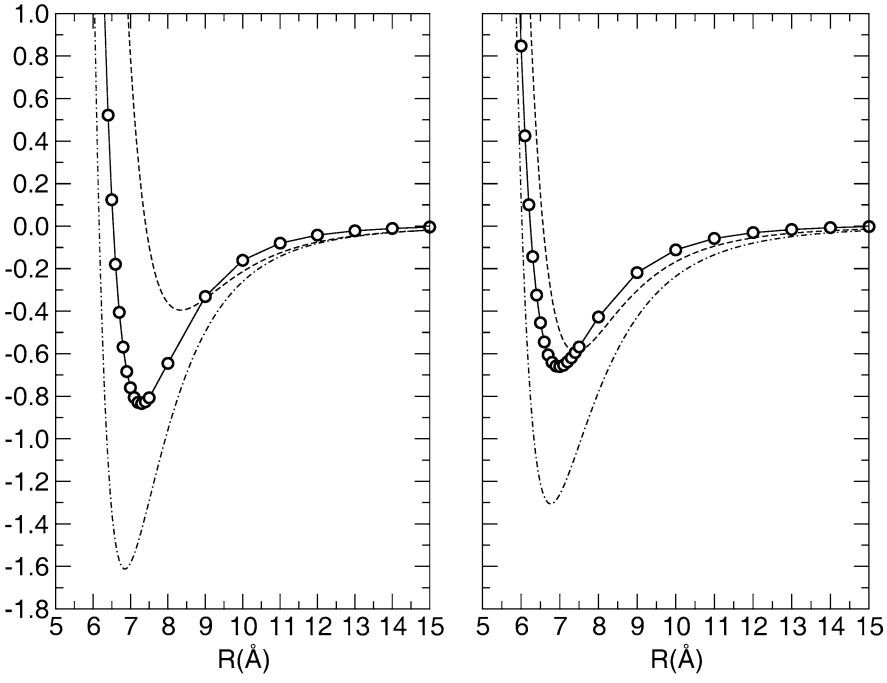

Fig. 3. Comparison of the attractive well of the potential: *circles* present work, *dashed line* from Ref. [13] and *dot-dashed* line from Ref. [14]. *Left panel* for $\theta = 0^\circ$, *right panel* for $\theta = 90^\circ$

BSSE in the calculations they used as input for the fitting. It is worth pointing out that the potential reported by Fuchs and Toennies has been improved by Gianturco et al. [15] to yield better vibrationally inelastic cross sections by adjusting some of the parameters in its analytical representation. The RR component was not, however, modified from the ones proposed before.

While differing substantially from previous empirical estimates, our potential shows here a shorter range of action and well depths that are intermediate with respect to previous results. It is nevertheless true for all existing PESs that they present a very weak angular anisotropy, a feature that is indeed relevant for the discussion of the rotational cooling collisions at ultralow energies already reported by us later [16]. To give an idea of the global behavior of this new PES we show a 3D view of it in Fig. 4. In that picture one can easily notice the mainly isotropic interaction and the well-defined molecular core identified by the repulsive region which shows no trace of any orientation-dependent molecular structure for this very weak Van der Waals complex.

The RR interaction potential was fitted to an analytic form in Jacobi coordinates for R larger than 2.5 Å. The potential is expanded in Legendre polynomials and, as mentioned before, it is essentially converged with the inclusion of $\lambda = 6$:

$$V_{\text{int}}(R,\theta) = \sum_{\lambda=0,2,4,6} V_\lambda(R) P_\lambda(\cos\theta) \tag{1}$$

where each coefficient $V_\lambda(R)$ (for $R < 15.0$ Å) has been fitted to the expression:

$$V_\lambda(R) = c_{\lambda,0}\frac{e^{-\alpha_\lambda R}}{R} + \sum_{i=1}^{9} c_{\lambda,i}\left(Re^{-\beta_\lambda R}\right)^i \tag{2}$$

For $R \geq 15.0$ Å each of the $V_\lambda(R)$ has been further analytically extended into the long-range region of interaction by extrapolating each of them through the usual perturbation expansion coefficients determined from the last few computed points:

$$V_\lambda(R) = \frac{C_6(\lambda)}{R^6} + \frac{C_8(\lambda)}{R^8} \tag{3}$$

The various coefficients of Eq. (2) are reported in Table 1.

3. Ultralow energy scattering

The de-excitation collisions that will be initially analyzed are the inelastic collisions occurring in the ultralow kinetic energy regime. In the entrance channel the molecule is taken to be in a rotationally excited state ($j = 0, 2, 4,$ and 6) and the open channels in the

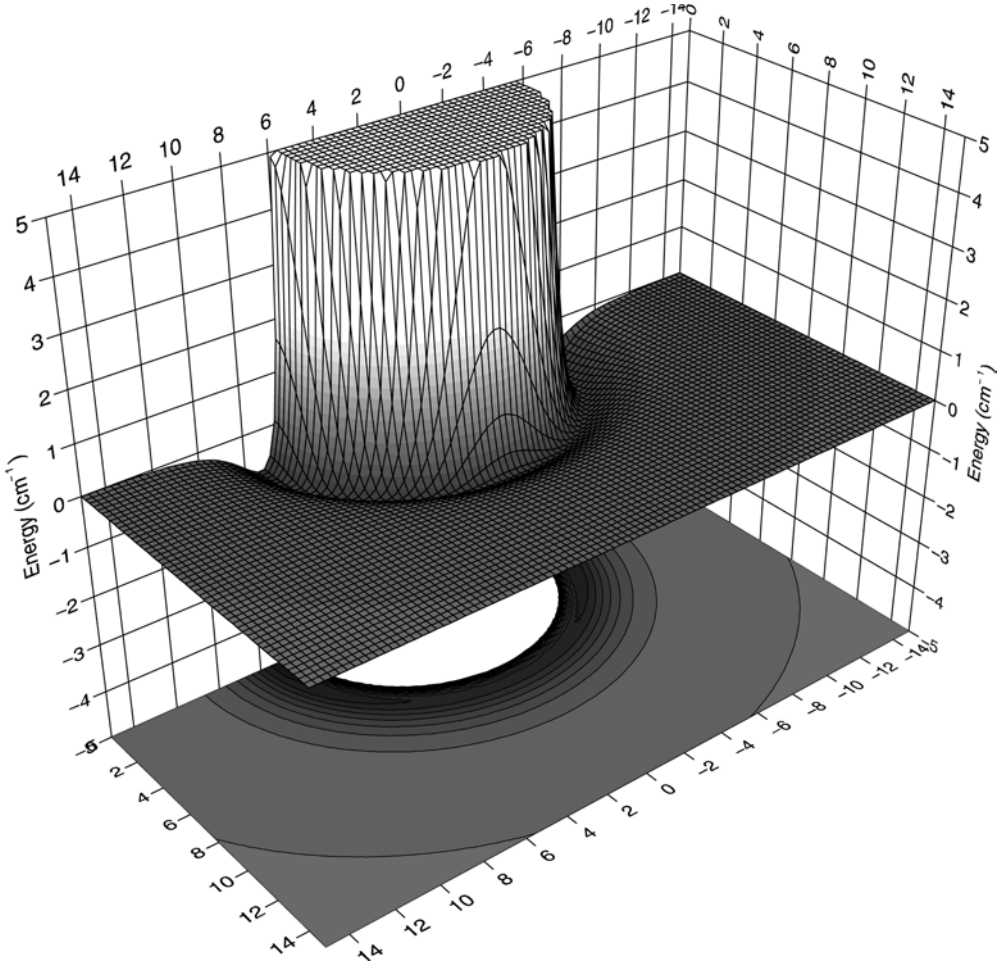

Fig. 4. 3D view of the interaction potential

Table 1. Coefficients for the analytic expression of the rigid rotor potential as a function of R ∈ [2.5,∞] Å and θ. Everything is in atomic units. Numbers in *parentheses* are the exponents of the decimal notation

	V_0	V_2	V_4	V_6
α	0.5	0.5	0.5	1.6218
β	0.5	0.5	0.5	1.0986
c_0	−0.870289(−1)	−0.183932(−1)	−0.138628(−1)	−0.206926(+3)
c_1	−0.602568(−3)	−0.517578(−4)	0.218747(−4)	0.873162(−3)
c_2	−0.118441(−1)	0.602994(−2)	0.402227(−2)	0.246637(+2)
c_3	0.502432	0.106773	−0.661691(−1)	0.964293(+3)
c_4	−0.414819(+1)	0.350547	0.148343(+1)	−0.744490(+3)
c_5	0.324000(+2)	−0.663623(+1)	−0.175986(+2)	0
c_6	−0.172160(+3)	0.130335(+2)	0.975611(+2)	0
c_7	0.541011(+3)	0.350719(+2)	−0.292743(+3)	0
c_8	−0.900533(+3)	−0.158505(+3)	0.456372(+3)	0
c_9	0.613186(+3)	0.180890(+3)	−0.254646(+3)	0
C_6	0.117870(+2)	0.216904(+1)	0.493947(−1)	−0.426189(−5)
C_8	−13557.9	−2358.83	−0.836376	0.003733

limit of zero initial kinetic energy are all the rotational levels with an energy less than ϵ_j. The time-independent formulation of any close coupling (CC) approach to quantum inelastic scattering is certainly well known and will be not repeated here. We will simply remind the reader of the basic form of the final CC equations leading to the final scattering states of the system [17, 18]:

$$\left\{\frac{\mathrm{d}^2}{\mathrm{d}R^2} + \mathbf{k}^2 - \mathbf{V} - \frac{\mathbf{l}^2}{R^2}\right\}\mathbf{G} = 0 \tag{4}$$

where $[\mathbf{k}^2]_{ij} = \delta_{ij} 2\mu(E - \epsilon_i)$ is the diagonal matrix of the asymptotic (squared) wavevectors, $\mathbf{V} = 2\mu\mathbf{U}$ is the potential coupling matrix, $[\mathbf{l}^2]_{ij} = \delta_{ij} l_i(l_i + 1)$ is the matrix representation of the square of the orbital angular momentum operator and $\mathbf{G}$ is the solution matrix which holds the radial channel components of the scattering wavefunction. From Eq. (4) we can extract the scattering matrix $\mathbf{S}$ by using the fact that in the asymptotic region the solution matrix can be written in the form

$$\mathbf{\Psi}(R) = \mathbf{J}(R) - \mathbf{N}(R) \cdot \mathbf{K} \ , \tag{5}$$

where $\mathbf{S} = (1 + i\mathbf{K})^{-1} \cdot (1 - i\mathbf{K})$ and where $\mathbf{J}(R)$ and $\mathbf{N}(R)$ are matrices of Riccati–Bessel and Riccati–Neumann functions. From the S matrix the inelastic cross sections can be finally obtained [17, 18]. Two problems, however, arise when dealing with ultralow collision energies: the large range of integration of the CC equations that is required and the number of steps requested by the integrator which become very large. We have recently published an algorithm for the solution of the CC equation [19] that modifies the variable phase approach in order to solve that problem addressing specifically the latter point.

Since the collision is inelastic (the molecule undergoes a relaxation from level j to a lower rotational level) the elastic phase shift is a complex number and we can define a complex scattering length as the limiting value of $\delta_j(k)/k$ when $k \to 0$, where k is the initial wavevector associated with the initial kinetic energy. Expanding the elastic element $S_{jj'}$ in powers of k we have [20]

$$S_{jj'} \simeq 1 + 2i\delta_j(k) = 1 - 2ik(\alpha_j - i\beta_j) = 1 - 2ika_j \ , \tag{6}$$

so knowledge of the elastic element of the $\mathbf{S}$ matrix when $k \to 0$ allows us to calculate the real (α_j) and imaginary (β_j) parts of the scattering length (a_j) [21, 22]. Total inelastic and elastic cross sections in the $k \to 0$ limit can then be easily calculated and are given by

$$\sigma_j^{el} = 4\pi|a_j|^2, \quad \sigma_j^{in} = \frac{4\pi\beta_j}{k} \ , \tag{7}$$

where the second expression is just the well-known Wigner threshold law for inelastic collisions. The usefulness of these expressions, originating from well-known threshold laws [20] employed in the case of multichannel scattering problems, can be easily understood in the context of the ultra-low energy quenching dynamics since the knowledge of the α and β quantities directly allows us to estimate from our calculations the collisional efficiency of such processes. The analytically continued $\mathbf{S}$ matrix has a pole at a point k_p located in the complex k-plane. We can thus obtain the complex energy value E_p of the resulting $\mathbf{S}$-matrix pole, on one of the two Riemann sheets of the two-fold complex energy plane, by using the formula

$$E_\mathrm{p} = \frac{k_p^2}{2\mu} = -\frac{\exp(i2\arctan(\beta_j/\alpha_j))}{2\mu|a_j|^2} = E - \frac{i}{2}\Gamma \ . \tag{8}$$

The real part of Eq. (8) gives the energy of the bound ($\alpha > 0$) or virtual ($\alpha < 0$) state. Since we are dealing with an inelastic collision because the initially excited molecule may undergo ro-vibrational quenching, the energy of the bound or virtual states has an associated width given by $\Im(E_\mathrm{p}) = \Gamma$, so the state becomes metastable and its lifetime is $\tau = 1/\Gamma$ [21].

4. Rotational de-excitation cross sections and scattering lengths

Rotationally inelastic cross sections were calculated and their ultralow energy behavior is reported in Fig. 5. The cross sections were obtained for various collision

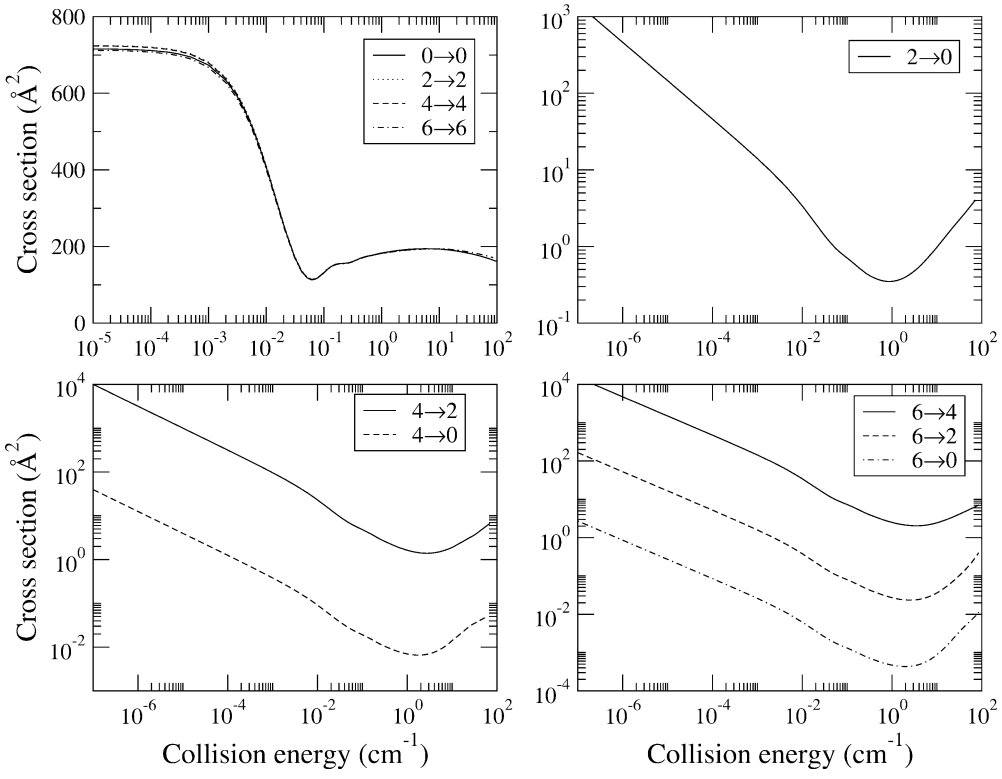

Fig. 5. Rotationally state-to-state elastic and inelastic cross sections as a function of collision energy and for different initial rotational states

energies starting from 10^{-5} up to 100 cm^{-1}. Owing to the small anisotropy of the interaction, the rotational basis that we employed was rather small and included the even-j states of the molecules up to $j_{max} = 10$. We integrated the coupled equations from 1 to 300 Å by employing a different number of total angular momentum values depending on the collision energy: the largest collision energy required 25 total angular momentum values to converge completely within less than 1%.

The top-left panel of Fig. 5. shows elastic cross sections for various initial j levels of the molecule: the four cross sections are very similar to each other and are very large in the ultralow energy limit. The weakness of the interaction potential makes the cross sections very smooth and without any sign of resonances even for energies larger than 1 cm^{-1} where centrifugal barriers often induce sharp shape resonances for systems that however exhibit stronger PES anisotropic features [16]. The only visible effect of a "resonant" behavior is the large value attained by the elastic cross section at very low energies. Indeed, this behavior is probably due to the presence of a virtual state near threshold because the scattering lengths associated with each initial j value turn out to be negative. The energy of this state can be estimated by the scattering length results to be about −0.3 cm^{-1} for each of the initial j levels. Since the interaction potential is so weak and the scattering is determined by the presence of the virtual state we can safely say that Li_2–He has no bound states. We also carried out further studies on the $Li_2(He)_n$ systems which will be presented elsewhere, with $n \leq 10$, and we found that all systems "classically" show small binding energies but the quantum effects prevent true bound states from appearing below $n = 3$. This is also the reason why we do not see any Feshbach resonance appearing at higher energies although the density of rotational states of Li_2 is relatively high. In an adiabatic picture Feshbach resonances are due to trapping of the wavefunction in the well generated by the presence of a closed channel whose energy is lowered locally (but not asymptotically) by the effect of the attractive interaction. None of the adiabatic potentials that we can obtain for different j values support bound states since the scattering length associated with the corresponding initial j value remains negative.

The various inelastic cross sections are reported in the further three panels of Fig. 5: for energies larger than 1 cm^{-1} the de-excitation cross sections are now 1 or 2 orders of magnitude smaller than the elastic ones because of the small angular anisotropy. At even smaller energies the cross sections start to diverge following Wigner's law. Given the extremely small rotational coupling in the present complex, the de-excitation cross section is chiefly controlled by the energy difference

Table 2. Scattering lengths, energies and zero temperature rate coefficents

Intial j state	α_j(Å^2)	β_j(Å^2)	Virtual state energy (cm^{-1})	De-excitation rate (cm^3 s^{-1})
0	−7.55	0	−0.095	0
2	−7.60	0.01	−0.094	1.17(−21)
4	−7.59	0.11	−0.094	8.06(−21)
6	−7.53	0.16	−0.096	1.21(−20)

between the rotational levels and therefore becomes larger when the initial energy content of the molecule is higher. On the whole, it is hard to expect that rotationally excited Li_2 molecules could be efficiently cooled by a He buffer gas at the energies expected to exist in the experiments[5].

The scattering lengths associated with each of the scattering processes, the energy of the virtual states detected in the present study, and the rate coefficient for the limit of zero temperature are reported in Table 2.

5 Conclusions

We have reported a new accurate PES that realistically describes the very weak van der Waals complex Li_2–He and its spatial region of interaction. This interaction was employed to obtain "exact" cross sections for the rotational transitions between the lowest states of the target diatomic. Generally speaking inelastic processes are usually weaker and inefficient with respect to elastic collisions unless the energy is extremely low and the Wigner regime has been reached. In this system we detected a very small rotational quenching rate for Li_2 compared with other systems with low angular anisotropy like CO–He [16, 23]. The scattering calculations discussed here allow us to obtain accurate elastic cross sections from which the scattering length can be obtained. Since the scattering length turns out to be negative and because of the very weak interaction within this complex we can conclude that the Li_2–He system does not support any bound state, at least with the PES calculated here, while it may become bound when interacting with more ^{4}He atoms as can occur "inside" the clusters generated by helium nanodroplets [24].

Acknowledgements. Financial support from the Italian Ministry for University and Research (MUIR), from the University of Rome "La Sapienza" Research Committee and from the INFM Computing Grant Committee is gratefully acknowledged.

References

1. Doyle J M, Friedrich B (1999) Nature 401: 749
2. Wynar R, Freeland R S, Han D J, Ryu C, Heinzen D J (2000) Science 287: 1016
3. Williams C, Julienne P (2000) Science 287: 986
4. Levi B G (2002) Phys Today 53: 46
5. Meijer G (2002) Chem Phys Chem 3: 495
6. Dion C, Drag C, Dulieu O, Tolra B L, Masnou-Seeuws F, Pillet P (2001) Phys Rev Lett 86: 2253
7. Tolra B L, Drag C, Pillet P (2001) Phys Rev A 64: 614101R
8. Bethlem L H, Berden G, Crompvoets F M H, Jongma R T, van Roij A J A, Meijer G (2000) Nature 406: 491
9. Weinstein J, deCarvalho R, Guillet T, Friedrich B, Doyle J M (1998) Nature 395: 148
10. Friedrich B, Weinstein J D, deCarvalho R, Doyle J (1999) J Chem Phys 110: 2376
11. Frisch M J, Trucks G W, Scuseria G E, Robb M A, Cheeseman J R, Zakrzewski V G, Montgomery J A, Jr Stratmann R E, Burant J C, Dapprich S et al. (1998) Gaussian 98, revision a.7. Guassian, Pittsburgh, PA
12. Kleinekathofer U, Lewerenz M, Mladenovich M (1999) Phys Rev Lett 83: 4717
13. Rubahn H G (1990) J Chem Phys 92: 5384
14. Fuchs M, Toennies J P (1986) J Chem Phys 85: 7062
15. Gianturco F A, Serna S, Delgado-Barrio G, Villareal P (1991) J Chem Phys 95: 5024
16. Bodo E, Gianturco F A (2003) J Phys Chem A 107: 7328
17. Taylor J R (1969) Scattering theory: the quantum theory of non-relativistic collisions. Krieger, Malabar, FL
18. Newton R G (1982) Scattering theory of waves and particles, 2nd edn. Springer, Berlin Herdelberg, New York
19. Martinazzo R, Bodo E, Gianturco F A (2003) Comput Phys Commun 151: 187
20. Landau L D, Lifshitz E M (1991) Quantum mechanics, vol 3, 3rd edn. Butterworth-Heinemann, Oxford
21. Balakrishnan N, Kharchenko V, Forrey R C, Dalgarno A (1997) Chem Phys Lett 280: 5
22. Balakrishnan N, Forrey R, Dalgarno A (1997) Chem Phys Lett 280: 1
23. Balakrishnan N, Dalgarno A, Forrey R C (2000) J Chem Phys 113: 321
24. Toennies J P, Vilesov A F (1998) Annu Rev Phys Chem 49: 1